SUPPLEMENTAL MATERIAL

Functional Gly297Ser Variant of the Physiological Dysglycemic Peptide Pancreastatin is a Novel Risk Factor for Cardiometabolic Disorders

by

Prasanna K. R. Allu[1,9], Malapaka Kiranmayi[1], Sromona D. Mukherjee[2], Venkat R. Chirasani[1], Richa Garg[3], Durairajpandian Vishnuprabu[4,10], Sudesh Ravi[4], Lakshmi Subramanian[1], Bhavani S. Sahu[1,11], Dhanya R. Iyer[1], Sakthisree Maghajoti[1], Saurabh Sharma[5], Marimuthu S. Ravi[6], Madhu Khullar[5], Arasambattu K. Munirajan[4], Jiaur R. Gayen[3], Sanjib Senapati[1], Ajit S. Mullasari[7], Viswanathan Mohan[8], Venkatesan Radha[8], Sathyamangala V. Naga Prasad[2] and Nitish R. Mahapatra[1]

Running title: Pancreastatin variant and cardiometabolic disorder

from the

[1]Department of Biotechnology, Bhupat and Jyoti Mehta School of Biosciences, Indian Institute of Technology Madras, Chennai 600036, India

[2]Department of Cardiovascular and Metabolic Sciences, Lerner Research Institute, Cleveland Clinic, Cleveland 44195, USA

[3]Pharmaceutics & Pharmacokinetics Division, CSIR-Central Drug Research Institute, Sector-10, Jankipuram Extension, Sitapur Road, Lucknow 226031, India

[4]Department of Genetics, Dr. ALM PG Institute of Basic Medical Sciences, University of Madras, Taramani Campus, Chennai 600113, India

[5]Department of Experimental Medicine and Biotechnology, Postgraduate Institute of Medical Education and Research, Chandigarh 160012, India

[6]Department of Cardiology, Madras Medical College and Government General Hospital, Chennai 600003, India

[7]Institute of Cardiovascular Diseases, Madras Medical Mission, Chennai 600037, India

[8]Department of Molecular Genetics, Madras Diabetes Research Foundation, Chennai 603103, India

[9]Present address: Section on Integrative Physiology and Metabolism, Joslin Diabetes Center, Harvard Medical School, Boston 02115, USA

[10]Present address: Center for Vascular and Inflammatory Diseases, University of Maryland Baltimore School of Medicine, Baltimore, Maryland 21201 USA

[11]Present address: National Brain Research Centre, Manesar, Gurugram, Haryana 122051, India

Correspondence should be addressed to:

Dr. Nitish R. Mahapatra, Department of Biotechnology, Bhupat and Jyoti Mehta School of Biosciences, Indian Institute of Technology Madras, Chennai 600036, India. Tel: 91-44-2257-4128; Fax: 91-44-2257-4102; E-mail: nmahapatra@iitm.ac.in

SUPPLEMENTARY INFORMATION

Human subjects and methodologies

We recruited 3602 unrelated volunteers from urban Chennai cosmopolitan population at three study centers: (i) Madras Diabetes Research Foundation [n=2464 subjects consisting of 1573 with hypertension (HTN) and/or type-2 diabetes (T2D) and/or intermediate glucose tolerance (IGT) and 891 healthy controls]; (ii) Madras Medical Mission (n=625 subjects with HTN/T2D); (iii) Madras Medical College [n=513 subjects with coronary artery disease (CAD)]. These three collection centers from Chennai mainly consisted of people from South Indian ancestry. We also recruited another group of unrelated subjects (n=716; consisting of 355 hypertensives and 361 normotensive controls) from North India at the Post Graduate Institute of Medical Education and Research, Chandigarh. The detailed demographic and clinical parameters are given in *SI Appendix* Tables S1 and S2.

In the overall population (Chennai and Chandigarh populations) (n=4318), the mean age of the subjects was ~48 years; ~27.2% of the subjects were type-2 diabetics; ~18.0% subjects were hypertensives; ~8.7% subjects had both T2D and HTN; ~5.1% had IGT; ~11.9% subjects had CAD; and ~29% subjects were healthy controls. The following criteria were adopted for disease classifications - diabetics: fasting blood sugar (FBS) ≥7.0 mmol/L (126 mg/dL), treatment with anti-diabetics drugs, or history of disease; hypertensives: systolic blood pressure (SBP) ≥140 mm Hg and/or diastolic blood pressure (DBP) ≥90 mm Hg or a history of hypertension and anti-hypertensive treatments; CAD: subjects with at least one block in their coronary artery or initial stage of myocardial infarction based on findings from angiogram and electro/echo-cardiogram. Normotensives served as the control subjects for hypertensives, while individuals with normal glucose tolerance served as controls for type-2 diabetics. All the

controls had no history of disease and medication. None of the subjects had kidney disease or any type of cancer.

Demographic (age, gender), physical [height, weight, body mass index (BMI)] and physiological parameters [SBP, DBP, mean arterial pressure (MAP)], medication status and blood samples [in ethylenediaminetetraacetic acid (EDTA)-containing tubes] were collected from the study subjects. Plasma samples were also collected, aliquoted and stored at -80°C. Genomic DNA from the subjects was isolated as described previously (1). Exon-7 region of *CHGA* was PCR-amplified, purified and sequenced to detect the presence of single nucleotide polymorphisms (SNPs) in the pancreastatin (PST) domains in the first set of samples, as described previously (2). The next set of DNA samples was genotyped for the p.Gly297Ser SNP (rs9658664) using PCR-mediated allelic discrimination method (*SI Appendix* Fig. S1); 5.0 µL reaction mixture contained 10 ng of genomic DNA, 2.5 µL of 2× TaqMan® Universal PCR master mix (Applied Biosystems, Waltham, MA, USA), 0.125 µL of 40× TaqMan® SNP genotyping assay mix (assay ID: C__25598362_10; containing 8 µM fluorescently-tagged probes specific for the wild-type and the variant alleles, 36 µM each of forward and reverse primers). PCR amplification conditions were according to the manufacturer's protocol: 2 min at 50°C, 10 min at 95°C, followed by 15 s at 92°C and 60 s at 60°C for 40 cycles. Allelic discrimination with end-point detection of fluorescence was carried out using ABI 7900HT sequence detection system followed by analysis with SDS software (Applied Biosystems). Non-template and positive controls were routinely included to ensure specificity and accuracy in genotyping.

Estimation of biochemical parameters

BMI was calculated by dividing the weight in kilograms with the square of the height in meters. Biochemical analyses were carried out on a Roche Cobas 8000 and Roche Cobas c702

Autoanalyzer. Blood glucose and cholesterol were measured using GOD-POD and CHOD-POD methods, respectively. Serum creatinine and urea were measured using creatinine amido hydrolase and urease methods, respectively. The blood pressure readings were made in the sitting position using a brachial oscillometric cuff by experienced nursing staff. Plasma PST levels in age-/sex-/BMI-matched diabetic and control subjects were measured using an enzyme-linked immunosorbent assay kit (that utilized an antibody raised against the PST domain of CHGA; catalog number: TM E-9000, LDN), according to the manufacturer's protocol.

Catecholamine secretion and glucose uptake assays

Briefly, SH-SY5Y and PC12 cells grown in poly-L-lysine-coated 12-well plates were incubated with 0.5 μCi of L-[7-^{3}H] norepinephrine (PerkinElmer, Waltham, MA, USA) in DMEM with 10% fetal bovine serum (FBS) (for SHSY-5Y), DMEM with 10% horse serum and 5% FBS (for PC12 cells) for 2 h at 37°C. Cells were washed twice with release buffer (150 mM NaCl, 5 mM KCl, 2 mM $CaCl_2$ and 10 mM HEPES pH 7.0) and then incubated with serum-free media for 30 min at 37°C. The cells were then treated with release buffer along with 100 nM of PST peptides (PST-WT or PST-297S). After 20 min of treatment with the peptides, the secretion media was collected and the cells were lysed with lysis buffer [*i.e.*, release buffer plus 0.1% (v/v) Triton™ X-100]. Secretion media and cell lysates were assayed for [^{3}H]-norepinephrine counts using a Tricarb™ liquid scintillation counter (PerkinElmer) and the results have been expressed as % secretion: (amount released/[amount released+amount in cell lysates]) × 100.

Estimation of glucose uptake by differentiated L6 and 3T3-L1 cells was carried out using a modified version of our previously reported protocol (2). In brief, cells were serum starved for 2 h and incubated in Krebs-Ringer HEPES buffer (120 mM NaCl, 5 mM KCl, 1.2 mM

$MgSO_4$, 1.3 mM $CaCl_2$, 1.3 mM KH_2PO_4 and 20 mM HEPES pH 7.4) without glucose in the presence or absence of 100 nM of PST peptides (PST-WT or PST-297S) for 10 min before stimulation with 20 nM insulin for 20 min. The cells were then incubated with 0.5 µCi [^{3}H]-2-deoxy-D-glucose (PerkinElmer) for an additional 20 min. Cells were washed with ice-cold phosphate-buffered saline (PBS), lysed with 0.5 M NaOH and 0.1% SDS, following which the radioactivity in the cell lysates was measured. Total protein was estimated using the Bradford method.

RNA extraction and real-time PCR

To estimate endogenous phosphoenol pyruvate carboxykinase-1 (*PCK1)* transcript, real-time PCR was performed using the DyNAmo™ HS SYBR® Green qPCR Kit (Thermo Fisher Scientific) and human *PCK1* specific primers: forward, 5'-GAGAAAGCGTTCAATGCCA-3' and reverse, 5'-ACGTAGGGTGAATCCGTCAG-3'. Similarly, to estimate endogenous glucose-6-phosphatase (*G6PC1*), the following primers were used: forward, 5'-TGCCCCTGATAAAGCAGTTC-3' and reverse, 5'-GGTCGGCTTTATCTTTCCCT-3'. For normalization of the expression levels of human *PCK1* and *G6PC1* genes, *β-actin* abundance was measured using the following primers: forward, 5'-CTGGTGCCTGGGGCG-3' and reverse, 5'-AGCCTCGCCTTTGCCGA-3'. The relative gene expression levels of both the genes were determined using the $2^{-\Delta\Delta Ct}$ method.

In this study, we have carried out cellular assays in different cell lines – HepG2, L6, SHSY-5Y, 3T3-L1 and PC12. The expression of *IR* and *GRP78* in all these cell lines has been reported previously – HepG2 (https://www.proteinatlas.org/ENSG00000044574-HSPA5/cell), L6 [IR: (3) and GRP78: (4)], SHSY-5Y (www.proteinatlas.org), 3T3-L1 [IR: (5) and GRP78: (6)] and PC12 [IR: (7) and GRP78: (8,9)]. In addition, using quantitative PCR, we found *GRP78* to be expressed in HepG2, L6 and SHSY-5Y as well (*SI Appendix* Fig. S6). Total RNA

samples from HepG2, SHSY-5Y and L6 cells were isolated as described previously (10). To estimate the endogenous *GRP78* transcript, real-time PCR was performed using the DyNAmo™ HS SYBR® Green qPCR Kit and human *GRP78* specific primers: forward, 5′-GGAAAGAAGGTTACCCATGC-3′ and reverse, 5′-AGAAGAGACACATCGAAGGT-3′ for the human cell lines, HepG2 and SHSY-5Y and rat GRP78 specific primers: forward, 5′-GAAACTGCCGAGGCGTAT-3′ and reverse, 5′-ATGTTCTTCTCTCCCTCTCTCTTA-3′ for the rat cell line L6. For normalization of human *GRP78* gene expression, *β-actin* abundance was measured using the following primers: forward, 5′-CTGGTGCCTGGGGCG-3′ and reverse 5′-AGCCTCGCCTTTGCCGA-3′. For normalization of rat *GRP78* gene expression, *β-actin* abundance was measured using the following primers: forward, 5′-GCTGTGCTATGTTGCCCTAG-3′ and reverse, 5′-CGCTCATTGCCGATAGTG-3′. The relative gene expression levels were determined using the $2^{-\Delta\Delta Ct}$ method.

GRP78 ATPase activity

To compare the effect of PST-WT and PST-297S on GRP78 ATPase activity, we performed spectrophotometric assay using recombinant human GRP78 protein (catalog no. ab78432, Abcam, Cambridge, MA, USA). PST-WT or PST-297S (2 µM) was co-incubated with GRP78 (1 µM) in 50 µL of assay buffer (20 mM Tris pH 7.5, 50 mM KCl and 1.5 mM $MgCl_2$) along with GRP78 alone in control wells. The reaction was started by adding 400 µM ATP and incubated at 37°C for 1 h. Liberated free phosphate (Pi) was measured using Malachite green-phosphate assay (catalog no. MAK307, Sigma-Aldrich, St. Louis, MO, USA) (n=4).

GRP78 expression study in HepG2 cells

To determine the inhibitory effect of PST-WT and PST-297S peptides on tunicamycin-stimulated GRP78 expression in HepG2 cells, we performed western blot. HepG2 cells were

cultured in 60-mm culture dishes. Upon reaching 80% confluence, the cells were treated with PST-WT or PST-297S (100 nM) along with tunicamycin (5 µg/mL) or with tunicamycin (5 µg/mL) alone for 24 h. No treatment was given in the control wells. After treatment, the cells were lysed in lysis buffer containing phosphatase and protease inhibitors. After separating equal amounts of protein using 10% sodium dodecyl sulfate-polyacrylamide gel electrophoresis (SDS-PAGE), gels were transferred to a polyvinylidene difluoride (PVDF) membrane. The non-specific binding proteins on the membrane were blocked using 5% skim milk powder in PBS with Tween (PBST; 2 h, room temperature). Membranes were then probed with the primary antibody, anti-GRP78 Bip (clone C50B12, Cell Signaling Technology, Danvers, MA, USA) at a dilution of 1:1000 dilution in PBST, overnight at 4°C. After five washes with PBST, the membranes were incubated with HRP-conjugated anti-rabbit secondary IgG at a dilution of 1:3000 for 2 h at room temperature. After five washes, the blots were visualized using ECL detection kit (cat no. WBKLS0500, Immobilon Western Chemiluminescent HRP Substrate, Merck Millipore, Darmstadt, Germany). The signals (n=5) were normalized with β-actin and the blots were analyzed using ImageJ software (NIH, Bethesda, MD, USA).

Generation of constructs for insulin receptor (IR) and glucose-regulated protein 78 (GRP78) overexpression

IR-FLAG and GRP78-FLAG overexpressing constructs were generated by cloning IR cDNA (a kind gift from Dr. Frederick M. Stanley) and GRP78 cDNA (catalog no. 32701, Addgene, Watertown, MA, USA) flanked by the restriction sites HindIII and XbaI at the 5' and 3' ends, respectively into the MCS of pcDNA 3.1. The primers were designed such that post-cloning the recombinant plasmids expressed IR and GRP78 with a FLAG tag at the C-terminal and N-terminal, respectively. The following primers were used for cloning: IR-FP: 5'-

CCCAAGCTTATGCACCTGTACCCCGGAGAG-3', IR-RP: 5'-GCTCTAGATTA**CTTGTCGTCATCGTCTTTGTAGTC**GGAAGGATTGGACCGAGG-3', GRP78-FP: 5'-CCCAAGCTTATG**GACTACAAAGACGATGACGACAAG**ATGAAGCTCTCCCTGGTG-3' and GRP78-RP: 5'-GCTCTAGACTACAACTCATCTTTTTCTGCTG-3'. The clones generated were confirmed using Sanger sequencing. The bold and underlined nucleotides indicate the FLAG coding sequences.

The IR-FLAG and GRP-FLAG overexpressing plasmids were transformed into DH5α cells using heat shock protocol and the transformed cells were plated on ampicillin-containing plates. Couple of colonies were selected and inoculated for mini-preparation of the plasmid. The plasmid sequence was authenticated using sequencing. Following authentication, large-scale preparation of the plasmids was performed and used for transfection into HEK-293 cells. HEK-293 cells used for the binding assays were cultured in Minimal Essential Media supplemented with 10% FBS and appropriate antibiotics. To assess the expression, increasing concentrations of the plasmids were transfected to determine the optimum concentration required for robust expression of the GRP78 and IR proteins. Cells were transfected with either GRP78- or IR-overexpressing constructs (8 μg/100 mm tissue culture dish) using TurboFect™ (Thermo Fisher Scientific) transfection reagent. 48 h following transfection, the cells were serum starved for 6 h before being used for each of the individual experiments.

Plasma membrane extraction and western immunoblotting

β-TC-6 cells were cultured in DMEM with high glucose supplemented with 15% heat-inactivated FBS and 1× penicillin/streptomycin. β-TC-6 cells (2.5×10^6) were plated on 150 mm tissue culture dishes and cultured by changing the medium every 24 h for 3 d (~60% confluency). Isolation of plasma membrane fraction (from HEK-293 and β-TC-6 cells) and

western immunoblotting was performed as previously described (11). Briefly, the cells were scraped using ice-cold non-detergent lysis buffer (5 mM Tris-HCl pH 7.4, 5 mM EDTA, 1 mM phenylmethylsulfonyl fluoride and 2 μg/mL of protease inhibitors leupeptin and aprotinin). The cells were dounced, toggled for 30 min at 4°C and centrifuged at 2500 rpm for 5 min at 4°C to remove cell debris and nuclei. The supernatant was centrifuged at 37,000 ×*g* for 30 min at 4°C. The pellet containing the plasma membrane was re-suspended in binding buffer (75 mM Tris-HCl pH 7.5, 2 mM EDTA and 12.5 mM $MgCl_2$) and protein estimation was performed using standard DC protein estimation (Bio-Rad, Hercules, CA, USA). 80 μg of the plasma membranes were resolved on an SDS-PAGE gel and transferred to a PVDF membrane for western immunoblotting.

Generation of PST peptide structures and docking with IR and GRP78

Molecular modeling of 52-mer PST-WT and PST-297S peptides was carried out using MODELLER program version 9v13 (12) with the previously derived 29-mer PST peptide structures (2) as templates because crystal or nuclear magnetic resonance structures of these peptides are not available. Initially, the PST-WT 52-mer and PST-WT 29-mer peptide sequences were aligned. On the basis of this alignment output and using the 29-mer PST peptide structure as a template, the PST-WT 52-mer structure was generated using MODELLER. Subsequently, Gly-297 was mutated to Ser-297 to generate the PST-297S peptide structure. The detailed methodologies for selecting the best models for wild-type and variant peptides from all the models generated by MODELLER have been presented (2). To mimic the physiological conditions, the modeled 52-mer PST-WT and PST-297S peptides were amide capped at the C-terminal end. The homology-modeled structures were further refined using molecular dynamics (MD) simulations for 200 ns. The stability of the simulated structures was assessed by plotting root mean square deviations (RMSD) of C_α atoms with

respect to the starting structure over the simulation period. The best models have all residues in allowed region of the Ramachandran plot. While RMSD for the PST-WT showed major fluctuations during the initial 80-90 ns, the PST-297S peptide did not display such fluctuations throughout the simulation time; the mean RMSD values for PST-WT and PST-297S were more or less similar after 90 ns. We also analyzed the secondary structural elements during the MD simulation. Consistent with the RMSD pattern the PST-297S peptide showed more stable secondary structural content throughout the trajectory (data not shown). The % of conformations carrying α-helix differed between the two peptides: 65% for PST-WT and 80% for PST-297S.

We used the protein-docking program, ZDOCK, to predict the binding of PST peptides to GRP78 monomer or IR. ZDOCK performs efficient global docking search on a 3D grid by using Fast Fourier Transform algorithm and scores docked complexes based on a combination of shape complementarity, electrostatics and statistical potential terms (13). ZDOCK predicted 100 binding modes of PST peptides with GRP78 and IR and these docked complexes were ranked according to ZDOCK score. Molecular interactions between PST peptides and GRP78 or IR were calculated using PDBsum database (14). ZDOCK scores between GRP78 and PST peptides were calculated by using ZDOCK 3.0.2. The binding energies (ΔG) and dissociation constants (K_d) between GRP78/IR and PST peptides were calculated using Protein-Protein Affinity Predictor (PPA-Pred) program (15). All the figures were rendered using PyMOL (The PyMOL Molecular Graphics System, version 1.5.0.4 Schrödinger, LLC).

SUPPLEMENTAL FIGURES

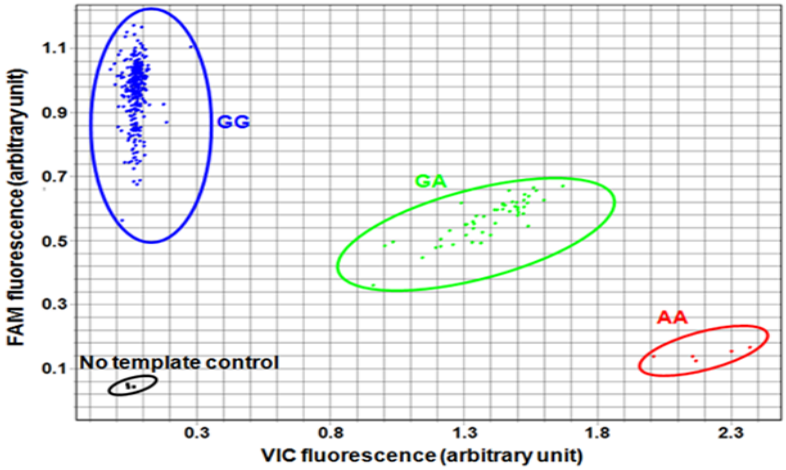

Fig. S1 Representative amplification plot for genotyping of the p.Gly297Ser polymorphism using TaqMan allelic discrimination method. Occurrence of G9358A SNP (rs9658664) that causes substitution of Gly by Ser at the 297th residue of the protein (*i.e.*, the PST p.Gly297Ser variation) was analyzed using the allele discrimination method. Representative amplification plot demonstrates the segregation of the GG, GA, AA genotypes and no template control. A substantial increase in only VIC-dye fluorescence indicated homozygosity for allele A (shown in red), a considerable increase in only FAM-dye fluorescence indicated homozygosity for allele G (shown in blue), while the presence of both VIC- and FAM-dye fluorescence indicated allele A-allele G heterozygosity (shown in green). SNP, single nucleotide polymorphism; PST, pancreastatin.

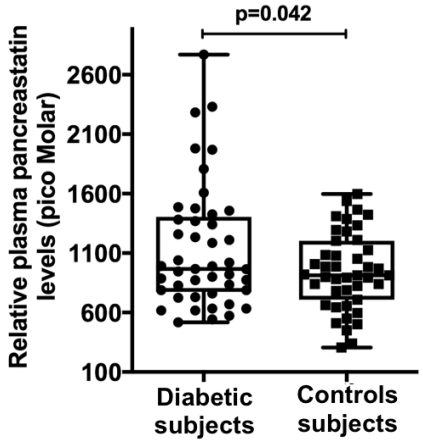

Fig. S2 Plasma PST levels are elevated in type-2 diabetic subjects. Plasma PST levels in freshly thawed plasma samples from age-/sex-/BMI-matched subjects were estimated using an ELISA kit. The relative plasma PST values have been expressed as mean ± S.D. Type-2 diabetic subjects (n=45) displayed ~20% higher plasma PST levels (p=0.042) as compared to control subjects (n=43) upon being compared using linear regression analysis. The BMI-adjusted p=0.043 and age-/BMI-adjusted p=0.041.

ELISA, enzyme-linked immunosorbent assay; PST, pancreastatin.

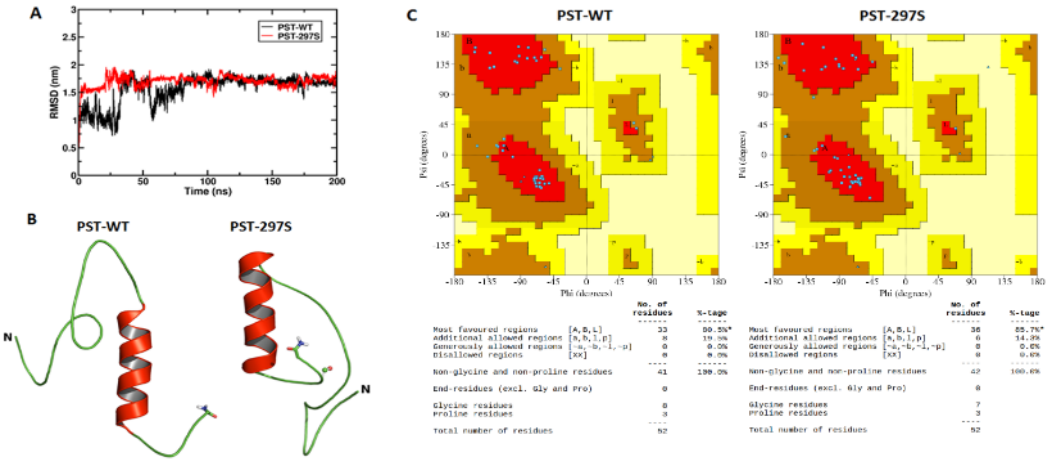

Fig. S3 Root mean square deviation analysis, modeled structures and Ramachandran plots of human PST peptides. (A) RMSD profiles of backbone atoms of human PST-WT (black) and variant PST-297S (red) peptides with respect to the corresponding starting structures were generated using g_rms module in Gromacs-4.5.5. RMSD values have been shown as a function of time (ns). The PST-WT peptide got stabilized and reached a plateau state within the first 80 ns; on the other hand, the PST-297S peptide stabilized and reached a plateau within the first 40 ns. Homology-modeled structures of PST-WT and its variant PST-297S were optimized, equilibrated and simulated for 200 ns. **(B)** Representative final snapshots of PST-WT and PST-297S peptides are shown as cartoons, the mutation sites are shown in ball and stick and the C-terminal amide capping is shown in licorice representation. **(C)** The quality of the modeled structures was analyzed using Procheck (16). Ramachandran plots for the PST-WT and PST-297S structures have about 80.5% and 85.7% of residues, respectively, in the most-allowed regions and no residues in the disallowed regions suggesting that the modeled structures are of good quality. Amino acid residues falling in the allowed region are represented using blue colored dots. The yellow, brown and red colored areas represent generously allowed, additionally allowed and most favored regions in the plot, respectively. Regions A, B and L correspond to the residues involved in the formation of right-handed α-helix, β-sheet and left-handed helix, respectively.

RMSD, root mean square deviation; PST: pancreastatin; PST-WT, wild-type pancreastatin peptide; PST-297S, variant pancreastatin peptide.

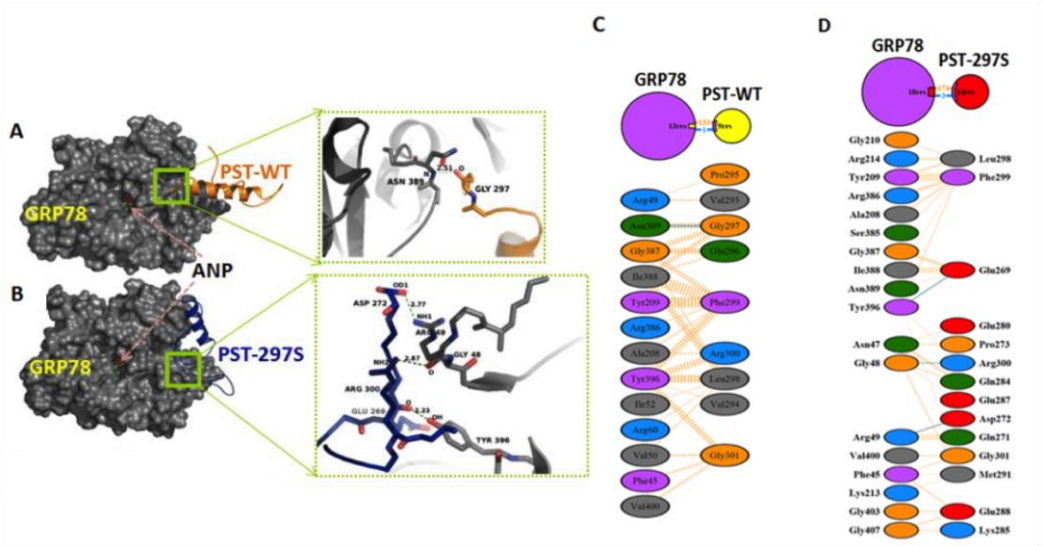

Fig. S4 Differential interactions of human PST peptides with GRP78. (A) A snapshot of the docked complex between PST-WT and GRP78. The hydrogen bond interaction (between Gly297 and Asn389) and atoms forming hydrogen bond are highlighted; PST-WT is shown in light orange color. **(B)** A snapshot of the docked complex between PST-297S and GRP78. Hydrogen bond interactions (between Glu269 and Tyr396; Arg300 and Gly48; Asp272 and Arg49) are highlighted and PST-297S is shown in blue color. GRP78 is shown in grey color. **(C)** PST-WT was found to interact with GRP78 via 1 hydrogen bond and 133 non-bonded contacts, the interacting residues are shown. **(D)** PST-297S was found to interact with GRP78 through 3 hydrogen bonds and 174 non-bonded contacts, the interacting residues are shown. The hydrophobic interactions have been represented using dotted lines, while hydrogen bonds have been represented using blue-colored lines.

PST, pancreastatin; PST-WT, wild-type pancreastatin peptide; PST-297S, variant pancreastatin peptide; GRP78, glucose-regulated protein 78.

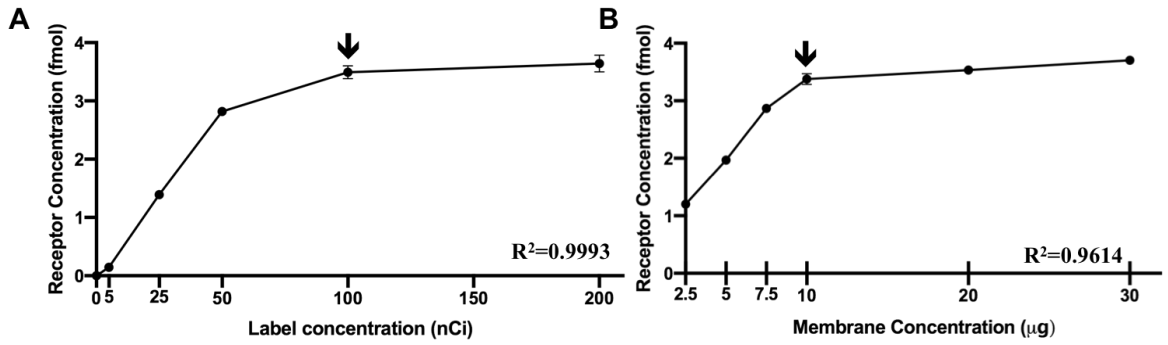

Fig. S5 Optimization of *in vitro* competitive binding experiments and comparison of the IR-binding abilities of PST peptides and insulin. (A) A binding assay with increasing concentrations of labeled PST (0, 5, 25, 50, 100 and 200 nCi) and 10 μg IR-expressing plasma membrane was performed in order to identify the optimal concentration of labeled $^{[125]}$I-Tyr PST to be used in the competitive binding experiments. **(B)** A binding assay with increasing amounts of IR-expressing plasma membrane (2.5, 5, 7.5, 10, 20 and 30 μg) and 100 nCi labeled $^{[125]}$I-Tyr PST was performed, to identify the optimal amount of IR-expressing plasma membrane to be used in the competitive binding experiments.

PST, pancreastatin; IR, insulin receptor.

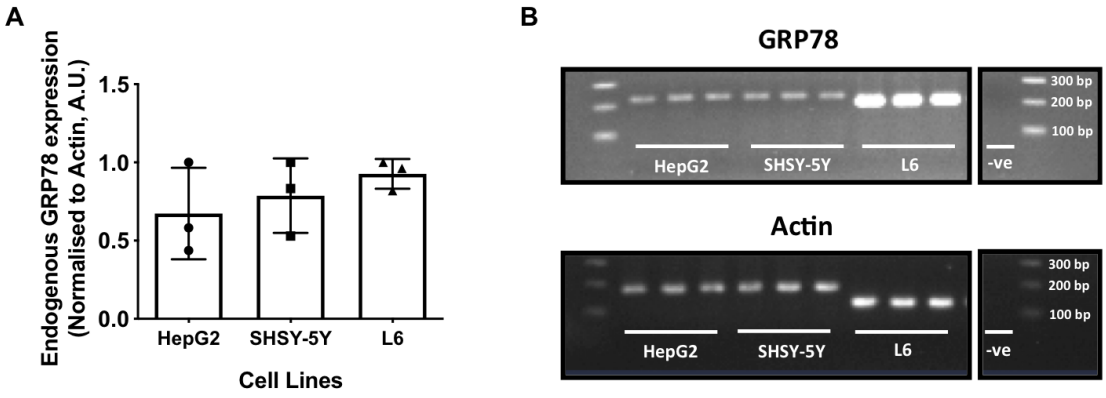

Fig. S6 Assessment of expression of GRP78 in the cell lines used in the study. (A) Relative abundance (expressed as arbitrary units) of human *GRP78* (in HepG2 and SHSY-5Y) and rat *GRP78* (in L6) was determined using quantitative RT-PCR. The *GRP78* mRNA levels were normalised to *β-actin* mRNA levels. **(B)** Gel picture showing the semi-quantitative PCR amplification of *GRP78* (top) and *β-actin* (bottom) using mRNA isolated from HepG2, SHSY-5Y and L6 cells as templates.

RT-PCR: real-time PCR, mRNA: messenger RNA.

SUPPLEMENTAL TABLES

Table S1 Demographic profile of the study subjects *

Study center/location	Parameter	Cases	Controls
MDRF (South India)	N	1573	891
	Age	52.0 ± 0.30	40.7 ± 0.42
	Male (%)/Female (%)	49.0%/51.0%	42.4%/57.6%
	Disease state		
	Type-2 diabetes	1110 (70.57%)	-
	Hypertension	34 (2.16%)	-
	Diabetes and hypertension	207 (13.16%)	
	Intermediate glucose tolerance	222 (14.11%)	-
MMM (South India)	N	625	-
	Age	41.3 ± 0.29	-
	Male (%)/Female (%)	73.3%/26.7%	-
	Disease state		
	Type-2 diabetes	65 (10.40%)	-
	Hypertension	390 (62.4%)	-
	Diabetes and hypertension	170 (27.2%)	-
MMC (South India)	N	513	-
	Age	51±0.49	
	Male (%)/Female (%)	87.10%/12.90%	-
	Disease state		
	Coronary artery disease	513 (100%)	-
PGIMER (North India)	N	355	361
	Age	45.8 ± 0.64	60.0 ± 0.40
	Male (%)/Female (%)	49.1%/50.9%	71.4%/28.6%
	Disease state		
	Hypertension	355 (100%)	-

* Subjects were recruited at four study centers: MDRF (Madras Diabetes Research Foundation, Chennai), MMM (Madras Medical Mission, Chennai), MMC (Madras Medical College, Chennai) and PGIMER (Post Graduate Institute of Medical Education and Research, Chandigarh). Majority of the subjects at the Chennai centers had South Indian ancestry while majority of the subjects at the Chandigarh center had North Indian ancestry. The values have been represented as mean ± S.E.M. Disease states of the cases are shown. Criteria for disease classifications were as follows. Type-2 diabetes - fasting blood sugar ≥7.0 mmol/L (126 mg/dL), treatment with anti-diabetic drugs or history of disease; hypertension: systolic blood pressure ≥140 mm Hg and/or diastolic blood pressure ≥90 mm Hg or history of hypertension and anti-hypertensive treatments; coronary artery disease: subjects with at least one block in

their coronary artery or initial stage of myocardial infarction based on findings from angiogram and electro/echo-cardiogram. Normotensives served as the control subjects for hypertensives, while individuals with normal glucose tolerance served as controls for diabetics. All the controls had no history of disease and medication. None of the subjects had kidney disease or any type of cancer.

Table S2 Clinical characteristics of case and control subjects *

Parameters	Cases	Controls	p-value
Physical			
Age (years)	48.95 ± 11.78 (n=3041)	46.30 ± 14.30 (n=1250)	<0.0001
BMI (kg/m^2)	25.45 ± 4.20 (n=2514)	24.07 ± 4.71 (n=887)	<0.0001
Physiological			
SBP (mm Hg)	132.19 ± 20.58 (n=2958)	118.35 ± 16.22 (n=1247)	<0.0001
DBP (mm Hg)	82.33 ± 12.27 (n=2958)	74.64 ± 10.18 (n=1247)	<0.0001
MAP (mm Hg)	98.95 ± 13.88 (n=2958)	89.20 ± 11.10 (n=1247)	<0.0001
Biochemical			
Urea (mg/dL)	23.32 ± 8.47 (n=2515)	21.03 ± 6.94 (n=886)	<0.0001
Creatinine (mg/dL)	0.85 ± 0.285 (n=2531)	0.85 ± 0.260 (n=886)	0.411
FBS (mg/dL)	143.01 ± 64.49 (n=1859)	87.37 ± 16.43 (n=867)	<0.0001
PGBS (mg/dL)	230.31 ± 100.87 (n=1800)	109.71 ± 33.74 (n=886)	<0.0001
FBS Insulin	11.46 ± 7.31 (n=572)	8.81 ± 6.06 (n=646)	<0.0001
PGBS Insulin	73.29 ± 60.06 (n=532)	61.92 ± 51.3 (n=499)	0.001
HOMA-IR index	3.81 ± 2.96 (n=571)	1.88 ± 1.36 (n=646)	<0.0001
HbA1c (%)	7.92 ± 2.31 (n=1485)	5.56 ± 0.65 (n=887)	<0.0001
TC (mg/dL)	185.82 ± 41.92 (n=2520)	177.38 ± 36.37 (n=887)	<0.0001
TG (mg/dL)	165.82 ± 121.90 (n=2521)	119.14 ± 82.13 (n=887)	<0.0001
HDL-C (mg/dL)	40.69 ± 9.41 (n=2461)	42.58 ± 9.70 (n=887)	<0.0001
LDL-C (mg/dL)	116.23 ± 35.76 (n=2391)	111.25 ± 31.11 (n=886)	<0.0001
VLDL-C (mg/dL)	32.26 ± 20.61 (n=1169)	23.02 ± 13.22 (n=867)	<0.0001

* Clinical parameters of the overall study population (Chennai and Chandigarh populations) (n=4318) stratified as cases and controls were analyzed using independent samples t-test. Values have been expressed as mean ± S.D. BMI, body mass index; SBP, systolic blood pressure; DBP, diastolic blood pressure; MAP, mean arterial pressure; FBS, fasting blood sugar; PGBS, post-glucose blood sugar; HOMA-IR index, insulin resistance index [fasting insulin (mIU/L) × fasting glucose (mg/dL)/405]; HbA1c, glycosylated hemoglobin; TC, total cholesterol; TG, triglycerides; HDL-C, high-density lipoprotein cholesterol; LDL-C, low-density lipoprotein cholesterol; VLDL-C, very low-density lipoprotein cholesterol.

Table S3 Statistical power of the study *

Disease state	Power of the study
Type-2 Diabetes	0.6839
Hypertension	0.7127
Coronary Artery Disease	0.6980
Metabolic Syndrome	0.9071

* Power of the study was analyzed using Quanto version 1.2.4 (17). By using case-control design/outcome and population risk as disease risk, the power of the sample size was calculated with 0.05 as the type 1 error rate. Statistical power of the study was calculated for all disease states (type-2 diabetes, hypertension, coronary artery disease and metabolic syndrome) involved in our study and the values are shown.

Table S4 Distribution PST p.Gly297Ser variant genotypes in different ethnic populations*

Ethnicity/Study		European	African	American	East Asian	South Asian	F_{ST} Score
1000 Genomes	N	1006	1322	694	1008	978	0.0377
	MAF (%)	0.89	0.08	0.00	0.00	5.80	
ExAC	N	9500	2882	464	858	7970	0.0355
	MAF (%)	1.45	0.21	1.51	0.12	8.57	
GnomAD-Genomes	N	18844	8690	848	1560	NA	0.0023
	MAF (%)	0.94	0.15	0.47	0.00	NA	
GnomAD-Exomes	N	78196	9174	24928	11780	22960	0.0420
	MAF (%)	0.94	0.16	0.43	0.02	8.33	
HapMap	N	176	298	592	168	NA	0.0115
	MAF (%)	1.10	0.30	3.20	0.00	NA	
ALFA	N	117750	3708	1788	324	62	0.0006
	MAF (%)	0.99	0.32	0.61	0.00	10.00	
PAGE Study	N	NA	NA	68744	8218	838	0.0128
	MAF (%)	NA	NA	0.32	0.06	6.80	
GenomeAsia 100K	N	228	208	52	1394	1448	0.0278
	MAF (%)	0.89	0.00	0.00	0.50	6.15	
Mean	MAF (%)	0.99	0.18	0.37	0.06	8.19	0.0334

* MAFs of the PST p.Gly297Ser variation (rs9658664) in various populations of the world, as calculated in different studies. The MAFs differed by ethnicity (χ^2=13688, p<0.0001). Of note, South Asian populations showed much higher MAFs than other populations. Data from the ExAC, GnomAD-Genomes and GnomAD-Exomes studies have been obtained from https://gnomad.broadinstitute.org/. Data for the 1000 genomes, HapMap, ALFA and PAGE studies have been obtained from dbSNP. Data for the GenomeAsia 100K study was taken from https://browser.genomeasia100k.org/. In the PAGE study, African American, Mexican, Puerto Rican, Native Hawaiian, Cuban, Dominican, Central American, South American and Native American populations have been considered as American. In the ALFA study, Latin American 1 and 2 populations have been considered as American. In the GenomeAsia 100k study,

Southeast Asian and Northeast Asian populations have been considered as East Asian. The global F_{ST} scores of the PST-G297 variant were calculated for the five major world populations from several studies, using the previously described equation (with all figures rounded off to fourth place after decimal):

$$F_{ST} = \frac{H_T - H_S}{H_T} \text{ with } H_T = 2 \times p \times q,\ H_S = \frac{H_{S1} * n_{s1} + H_{S2} * n_{s2}}{n_{s1} + n_{s2}},\ \text{and } H_{Si} = 2 \times p_{Si} \times q_{Si} \quad (18),$$

where p_{Si} and q_{Si} are the allele frequencies in subpopulation i, n_{s1} and n_{s2} are the number of individuals of the subpopulations S_1 and S_2, respectively, H_S is the average heterozygosity of the subpopulations and H_T is the heterozygosity based on the total population. F_{ST} values below 0.05 indicate low differentiation (*i.e.*, negative selection pressure) and values above 0.65 indicate extreme differentiation (*i.e.*, positive selection pressure) (19). All the studies had F_{ST} values <0.05, suggesting that the altered function arising as a consequence of this variant results in it being selected against, hence leading to little genetic differentiation.

MAF, minor allelic frequency; GnomAd, genome aggregation database; ExAC, exome aggregation consortium; ALFA, allele frequency aggregator; PAGE, population architecture using genomics and epidemiology; NA, data not available.

Table S5 Extent of interactions of the PST peptides with GRP78 and IR*

Ligand-receptor complex	Binding free energy (ΔG) (Kcal/mole)	Dissociation constant (K_d) (M)
Insulin and insulin receptor	-12.32	9.22×10^{-10}
PST-WT and insulin receptor	-12.02	15.3×10^{-10}
PST-297S and insulin receptor	-12.40	8.06×10^{-10}
PST-WT and GRP78	-7.89	1.64×10^{-6}
PST-297S and GRP78	-9.18	0.185×10^{-6}

* Binding free energy and dissociation constant values were calculated using PPA-Pred program (15).

PST, pancreastatin; PST-WT, wild-type pancreastatin peptide; PST-297S, variant pancreastatin peptide; GRP78, glucose-regulated protein 78; IR, insulin receptor

Table S6 GWAS-identified associations of rs9658664 with disease conditions*

Disease	Odds ratio	p-value	Direction of effect	Study	Sample Size (n)
T2D	1.127	0.1	↑	DIAGRAM 1000G GWAS	82594
T2D adj BMI	**1.234**	**0.024**	↑		**56443**
Claudication in T2D	2.140	0.134	↑	BioMe AMP T2D GWAS	1095
PVD in T2D	**2.588**	**0.038**	↑		**1350**
Stroke in T2D	2.074	0.162	↑		790
Hypertension in T2D	0.478	0.106	↓		1110
T2D	1.059	0.099	↑	DIAMANTE (European) T2D GWAS	231420

*The association of PST 297Ser allele with various cardiometabolic conditions has been tested in different GWAS studies carried out till date including DIAGRAM 1000G GWAS (20), BioMe AMP T2D GWAS (21–24) and DIAMANTE (European) T2D GWAS (25). Data for generating this figure have been obtained from https://t2d.hugeamp.org/ as accessed on 15th March 2021.

T2D, type-2 diabetes; BMI, body mass index; PVD, peripheral vascular disease; CAD, coronary artery disease; MI, myocardial infarction

SUPPLEMENTARY REFERENCES

1. Sahu BS, Obbineni JM, Sahu G, Allu PKR, Subramanian L, Sonawane PJ, et al. Functional genetic variants of the catecholamine-release-inhibitory peptide catestatin in an Indian population: Allele-specific effects on metabolic traits. J Biol Chem. 2012;287(52):43840–52.
2. Allu PKR, Chirasani VR, Ghosh D, Mani A, Bera AK, Maji SK, et al. Naturally occurring variants of the dysglycemic peptide pancreastatin: Differential potencies for multiple cellular functions and structure-function correlation. J Biol Chem. 2014;289(7):4455–69.
3. Egawa K, Maegawa H, Shimizu S, Morino K, Nishio Y, Bryer-Ash M, et al. Protein-tyrosine Phosphatase-1B Negatively Regulates Insulin Signaling in L6 Myocytes and Fao Hepatoma Cells. J Biol Chem. 2001;276(13):10207–11.
4. Ebersbach-Silva P, Poletto AC, David-Silva A, Seraphim PM, Anhê GF, Passarelli M, et al. Palmitate-induced Slc2a4/GLUT4 downregulation in L6 muscle cells: Evidence of inflammatory and endoplasmic reticulum stress involvement. Lipids Health Dis. 2018;17(1):64.
5. Kim WJ, Lee W, Jung Y, Jang hyuk J, Kim YK, Kim SN. PPARβ/δ agonist GW501516 inhibits TNFα-induced repression of adiponectin and insulin receptor in 3T3-L1 adipocytes. Biochem Biophys Res Commun. 2019;510(4):621–8.
6. Kitzman HHJ, McMahon RJ, Aslanian AM, Fadia PM, Frost SC. Differential regulation of GRP78 and GLUT1 expression in 3T3-L1 adipocytes. Mol Cell Biochem. 1996 Sep;162(1):51–8.
7. Geetha T, Rege SD, Mathews SE, Meakin SO, White MF, Babu JR. Nerve growth factor receptor TrkA, a new receptor in insulin signaling pathway in PC12 cells. J Biol

Chem. 2013;288(33):23807–13.

8. Jing X, Shi Q, Bi W, Zeng Z, Liang Y, Wu X, et al. Rifampicin protects PC12 cells from rotenone-induced cytotoxicity by activating GRP78 via PERK-eIF2α-ATF4 pathway. PLoS One. 2014;9(3):e92110.
9. Zhang X-Y, Zhang T-T, Song D-D, Zhou J-H, Han R, Qin Z-H, et al. Endoplasmic reticulum chaperone GRP78 is involved in autophagy activation induced by ischemic preconditioning in neural cells. Mol Brain. 2015;8:20.
10. Sonawane PJ, Sahu BS, Sasi BK, Geedi P, Lenka G, Mahapatra NR. Functional promoter polymorphisms govern differential expression of HMG-CoA reductase gene in mouse models of essential hypertension. PLoS One. 2011;6(1):e16661.
11. Vasudevan NT, Mohan ML, Gupta MK, Hussain AK, Naga Prasad S V. Inhibition of protein phosphatase 2A activity by PI3Kgamma regulates beta-adrenergic receptor function. Mol Cell. 2011;41(6):636–48.
12. Eswar N, Webb B, Marti-Renom MA, Madhusudhan MS, Eramian D, Shen M-Y, et al. Comparative protein structure modeling using Modeller. Curr Protoc Bioinforma. 2006;Chapter 5:Unit-5.6.
13. Pierce BG, Hourai Y, Weng Z. Accelerating protein docking in ZDOCK using an advanced 3D convolution library. PLoS One. 2011;6(9):e24657.
14. de Beer TAP, Berka K, Thornton JM, Laskowski RA. PDBsum additions. Nucleic Acids Res. 2014;42:D292-6.
15. Yugandhar K, Gromiha MM. Feature selection and classification of protein-protein complexes based on their binding affinities using machine learning approaches. Proteins. 2014;82(9):2088–2096.
16. Laskowski RA, MacArthur MW, Moss DS, Thornton JM. PROCHECK: a program to check the stereochemical quality of protein structures. J Appl Crystallogr.

1993;26(2):283–91.

17. Gauderman WJ. Sample size requirements for matched case-control studies of gene-environment interaction. Stat Med. 2002;21(1):35–50.

18. Chang LY, Toghiani S, Hay EH, Aggrey SE, Rekaya R. A weighted genomic relationship matrix based on fixation index (Fst) prioritized SNPs for genomic selection. Genes (Basel). 2019;10(11):922.

19. Barreiro LB, Laval G, Quach H, Patin E, Quintana-Murci L. Natural selection has driven population differentiation in modern humans. Nat Genet. 2008;40:340–5.

20. Scott RA, Scott LJ, Mägi R, Marullo L, Gaulton KJ, Kaakinen M, et al. An Expanded Genome-Wide Association Study of Type 2 Diabetes in Europeans. Diabetes. 2017;66(11):2888–902.

21. Gaulton KJ, Ferreira T, Lee Y, Raimondo A, Mägi R, Reschen ME, et al. Genetic fine mapping and genomic annotation defines causal mechanisms at type 2 diabetes susceptibility loci. Nat Genet. 2015;47(12):1415–25.

22. Wessel J, Chu AY, Willems SM, Wang S, Yaghootkar H, Brody JA, et al. Low-frequency and rare exome chip variants associate with fasting glucose and type 2 diabetes susceptibility. Nat Commun. 2015;6:5897.

23. Ng MCY, Shriner D, Chen BH, Li J, Chen WM, Guo X, et al. Meta-Analysis of Genome-Wide Association Studies in African Americans Provides Insights into the Genetic Architecture of Type 2 Diabetes. PLoS Genet. 2014;10(8):e1004517.

24. Tayo BO, Teil M, Tong L, Qin H, Khitrov G, Zhang W, et al. Genetic background of patients from a university medical center in Manhattan: Implications for personalized medicine. PLoS One. 2011;6(5):e19166.

25. Mahajan A, Taliun D, Thurner M, Robertson NR, Torres JM, Rayner NW, et al. Fine-mapping type 2 diabetes loci to single-variant resolution using high-density imputation

and islet-specific epigenome maps. Nat Genet. 2018;50(11):1505–13.